



HAL
open science

Synthesis of a New Modification of Lithium Chloride Confirming Theoretical Predictions

Martin Jansen, Andreas Bach, Dieter Fischer

► **To cite this version:**

Martin Jansen, Andreas Bach, Dieter Fischer. Synthesis of a New Modification of Lithium Chloride Confirming Theoretical Predictions. *Journal of Inorganic and General Chemistry / Zeitschrift für anorganische und allgemeine Chemie*, 2009, 10.1002/zaac.200900357 . hal-00515815

HAL Id: hal-00515815

<https://hal.science/hal-00515815>

Submitted on 8 Sep 2010

HAL is a multi-disciplinary open access archive for the deposit and dissemination of scientific research documents, whether they are published or not. The documents may come from teaching and research institutions in France or abroad, or from public or private research centers.

L'archive ouverte pluridisciplinaire **HAL**, est destinée au dépôt et à la diffusion de documents scientifiques de niveau recherche, publiés ou non, émanant des établissements d'enseignement et de recherche français ou étrangers, des laboratoires publics ou privés.



Zeitschrift für Anorganische und
Allgemeine Chemie

Synthesis of a New Modification of Lithium Chloride Confirming Theoretical Predictions

| | |
|-------------------------------|---|
| Journal: | <i>Zeitschrift für Anorganische und Allgemeine Chemie</i> |
| Manuscript ID: | zaac.200900357 |
| Wiley - Manuscript type: | Article |
| Date Submitted by the Author: | 27-Jul-2009 |
| Complete List of Authors: | Jansen, Martin; MPI für Festkörperforschung Bach, Andreas; MPI fuer Festkoerperforschung, Chemie III Fischer, Dieter; MPI fuer Festkoerperforschung, Chemie III |
| Keywords: | lithium chloride, polymorphism, structure elucidation, wurtzite, atomic-beam-deposition |
| | |



1
2
3
4
5
6
7
8
9
10
11
12
13
14
15
16
17
18
19
20
21
22
23
24
25 **Synthesis of a New Modification of Lithium Chloride Confirming Theoretical**

26
27 **Predictions**
28
29
30
31
32

33
34 Andreas Bach, Dieter Fischer and Martin Jansen^{*}
35
36

37
38 Stuttgart/D, Max-Planck-Institut für Festkörperforschung
39
40
41

42
43 Received:
44
45
46
47
48
49
50
51
52

53
54
55 _____
56 * Prof. Dr. M. Jansen
57

58 Max-Planck-Institut für Festkörperforschung
59

60 Heisenbergstraße 1, 70569 Stuttgart/D

Fax: +49(0)711-6891502, E-Mail: M.Jansen@fkf.mpg.de

Abstract

In accordance with prior calculations, the new polymorph β -LiCl (wurtzite structure type) has been synthesized, via the low-temperature atomic-beam-deposition (LT-ABD) technique, in a mixture with α -LiCl (rock salt structure type) by depositing LiCl vapour (2 to $5.3 \cdot 10^{-4}$ mbar) onto a cooled substrate (-30 to -60 °C). The maximum β -LiCl fraction of 53 % was obtained using a sapphire (0001) substrate at -50 °C and $3.7 \cdot 10^{-4}$ mbar LiCl vapour pressure. The proportion of the new polymorph contained in the bulk sample decreases as temperature or vapour pressure deviate from these values, until finally the rock salt type LiCl is found exclusively. When warming the samples up to room temperature, β -LiCl irreversibly transforms to α -LiCl. The X-ray diffraction pattern of the two phase LiCl sample measured at -50 °C has been indexed and refined based on a hexagonal unit cell for β -LiCl with the lattice constants $a = 3.852(1)$ Å and $c = 6.118(1)$ Å and a cubic unit cell for α -LiCl with the lattice constant $a = 5.0630(8)$ Å. By Rietveld refinement the wurtzite type of structure ($P6_3mc$, No. 186) was suggested for the new hexagonal modification of LiCl with the Li-Cl distances (2.32 and 2.34 Å) being 8 % smaller than those of α -LiCl. Moreover the cell volume decreases as much as 16 % during the transition from β -LiCl to α -LiCl. Both the shifts in bond lengths and volume correspond well with the situation encountered for LiBr and LiI. Besides the variation of LiCl vapour pressure and substrate temperature, also different substrate materials were employed for testing their influence on formation of the β -LiCl polymorph.

Key words: lithium chloride, polymorphism, structure elucidation, wurtzite, atomic-beam-deposition

Introduction

Projecting the world of chemical matter onto an energy landscape associated to the respective configuration space constitutes the foundation of our approach to rational chemical synthesis [1-3]. There is a “one to one” relationship between the ensemble of chemical compounds capable of existence and the structure of the energy landscape: each compound corresponds to a (local) minimum on the landscape and vice versa. In the first step of synthesis planning the (meta)stable compounds of a given chemical subsystem are identified by globally exploring the related landscape, or more specifically, by identifying the minima. Realizing the predicted compounds, in particular the metastable ones, by chemical synthesis often turns out to be an intriguing task. Our approach of rational synthesis planning, the prediction and realization of new compounds, has proven to be rather efficient also with this respect [2], and among others, has enabled us to synthesize up to then elusive Na_3N [4].

Full exploration of the energy landscapes of the alkali metal halides has resulted in the prediction of many modifications to exist in addition to the known rock salt and CsCl types of structure [5]. For the lithium halides those modifications containing lithium in a tetrahedral coordination, i.e. zinc blende and wurtzite types, have turned out to be energetically competitive with the stable rock salt structures. Indeed, using the LT-ABD technique [6], $\beta\text{-LiI}$ and $\beta\text{-LiBr}$ have been realized in the hexagonal wurtzite structures, recently [7, 8]. These findings are in a certain sense complying with the traditional structure field diagrams based on radii ratios of hard sphere ions. Here the stability range for an octahedral coordination, i.e. of the rock salt type, is $0.414 \leq r_K/r_A \leq 0.732$. LiI and LiBr with $r_K/r_A = 0.35$ and 0.39 , respectively, are border line cases or even beyond this range [9]. In contrast, LiCl exhibiting a ratio of $r_K/r_A = 0.42$ is clearly

1
2
3 located within the stability range of the rock salt type. However, computational global
4 searches and ab initio optimization of the structure candidates [5] have shown that for
5
6
7
8 LiCl as well, the energies for the wurtzite and zinc blende modifications are rather low,
9
10 as one can deduce from the energy versus volume curves displayed in Fig. 1.

11
12 Here, we report on our experiments aiming at realizing LiCl in one of the predicted
13
14
15 metastable modifications.
16
17
18
19
20
21

22 Results and Discussion

23
24 The deposition of LiCl onto various substrates at low temperatures via our LT-ABD
25
26 technique [6] resulted in transparent films which changed into white opaque when
27
28 warmed up to room temperature. With (0001)-oriented sapphire as substrate, the
29
30 parameter field of deposition was explored. In the temperature range of -30 to -60 °C
31
32 and vapour pressures from 2 to $5.3 \cdot 10^{-4}$ mbar the new polymorph β -LiCl, besides α -
33
34 LiCl, was found. The maximum β -LiCl fraction of 53 % was obtained at -50 °C
35
36 sapphire substrate temperature and $3.7 \cdot 10^{-4}$ mbar vapour pressure. The proportion of the
37
38 new polymorph in the sample decreases as temperature or vapour pressure deviate from
39
40 these optimal values. Finally, outside the parameter window given above for the
41
42 substrate temperature and the vapour pressure, only rock salt structure type α -LiCl is
43
44 found. The fractions of β - and α -LiCl (wt %) were calculated from Rietveld structure
45
46 refinements and are displayed in Fig. 2. Here, the percentaged crystalline fraction of
47
48 β -LiCl is shown as a function of substrate temperature and LiCl vapour pressure during
49
50 deposition for different substrate materials. When heating the sample, β -LiCl starts to
51
52 transform to α -LiCl around 0 °C with the phase transition completed at room
53
54 temperature (Fig. 3). The X-ray diffraction pattern of the two phase LiCl sample
55
56 measured at -50 °C has been indexed and refined based on a hexagonal unit cell for
57
58
59
60

1
2
3 β -LiCl ($a = 3.852(1) \text{ \AA}$; $c = 6.118(1) \text{ \AA}$) and the cubic unit cell for α -LiCl
4
5 ($a = 5.0630(8) \text{ \AA}$). For the purpose of calibration, we used the lattice constant of α -LiCl
6
7 at room temperature ($a = 5.131(1) \text{ \AA}$; Lit.: 5.132 \AA [11]). The two phase Rietveld
8
9 refinement, also addressing the effect of preferred orientation, suggested the wurtzite
10
11 structure type ($P6_3mc$, No. 186) for the new hexagonal modification of LiCl (Fig. 4)
12
13 with Li-Cl distances (2.32 and 2.34 \AA) being 8 % smaller than those of α -LiCl (Tab. 1).
14
15 Moreover the cell volume decreases as much as 16 % during the transition from β -LiCl
16
17 to α -LiCl. Both observations correspond well with the situation encountered for LiI and
18
19 LiBr [7, 8]. A comparison of the cell parameters and volumes for different lithium
20
21 halides shows that the results for LiCl in principle follow the trends as encountered for
22
23 (both α - and β -) lithium halides with heavier halogens (Fig. 5). However, the decrease
24
25 in volume for the cubic phases is larger as compared to the hexagonal ones.
26
27
28
29
30

31
32 The ratio of α -/ β -LiCl appeared to be laterally constant within individual preparations,
33
34 as monitored by X-ray diffraction. This is in accordance with the SEM pictures taken
35
36 from the sample surface (Fig. 6) which do not show any noticeable variations in lateral
37
38 direction. We attribute the microstructure observed to volume shrinkage at the transition
39
40 from α - to β -LiCl. An increase of the crystallite size with increasing substrate
41
42 temperature was observed. In addition to sapphire (0001), different surfaces of various
43
44 single crystal materials have been tested as substrates. When using ZnO (0001), NaCl
45
46 (111) and cleaved CaF_2 (111), no β -LiCl was generated. The experiments on ZnSe (111)
47
48 and CaF_2 (111) resulted in amounts of β -LiCl comparable to those on sapphire (0001)
49
50 substrates. Due to these results no direct relations seem to exist between the selected
51
52 substrate exposing a certain surface and the formation of β -LiCl. Hence, if at all, the
53
54 substrate surface only plays an inferior role for the emergence of hexagonal LiCl.
55
56
57
58

59
60 Furthermore, our results reveal a small window of synthesis parameter combinations
(substrate temperature and vapour pressure), where β -LiCl can be obtained, with the

1
2
3 substrate temperature being the more crucial factor of influence. In Fig. 2 is shown that
4
5 β -LiCl preferably forms at a substrate temperature of about $-45\text{ }^{\circ}\text{C}$. At a first glance it is
6
7 hard to rationalize that α - and β -LiCl crystallize simultaneously, and that the less stable
8
9 polymorph survives together with the more stable one. The formation of β -LiCl, quite
10
11 obviously, has thus to be attributed to non-equilibrium phenomena connected to the
12
13 otherwise rather selective steps of nucleation and growth. Commonly, during the
14
15 pre-stages of crystallization a dynamical population of subcritical nuclei develops, out
16
17 of which those start to grow that reach the critical size and stability first. In our
18
19 experiments, in a small temperature window local nucleation takes place at which the
20
21 seeds for the different structure types do not appear to equilibrate or to undergo the
22
23 common selection process. Instead of that, in the case of LiCl, seeds start growing with
24
25 the growth fed from the LiCl in the gas phase. If the substrate temperature is raised,
26
27 thermal activation favours the transformation to the global minimum structure, i.e. the
28
29 rock salt modification, and above $-30\text{ }^{\circ}\text{C}$ substrate temperature α -LiCl is obtained
30
31 exclusively. The parameter window is significantly smaller as compared to the cases of
32
33 β -LiBr and β -LiI [7, 8], and the temperature windows narrow from LiI (-196 to $0\text{ }^{\circ}\text{C}$) to
34
35 LiBr (-100 to $-20\text{ }^{\circ}\text{C}$) and LiCl (-60 to $-30\text{ }^{\circ}\text{C}$).
36
37
38
39
40
41
42

43 These results confirm the high potential of the LT-ABD technique as to the formation of
44
45 metastable compounds, though the parameter space needs to be explored very
46
47 accurately to obtain the targeted possible polymorphs, and the parameter window for
48
49 new polymorphs may be very small, like with LiCl.
50
51
52
53
54
55
56

57 Experimental Part

58 Lithium chloride (99,99 %, Aldrich) was dried at $200\text{ }^{\circ}\text{C}$ in vacuum and directly
59
60 evaporated from a home-made resistance heater (stenan crucible, Hoechst CeramTec

1
2
3 AG) which was held at a constant temperature between 450 and 490 °C, and deposited
4
5 onto a cooled substrate inside a ultra high vacuum chamber for a period of several
6
7 hours. Ultra high vacuum of $1 \cdot 10^{-8}$ to $5 \cdot 10^{-9}$ mbar was maintained during preparation in
8
9 the deposition chamber by using a turbo molecular and cryopump system including a
10
11 liquid nitrogen filled cold trap. The residual gas was analyzed and monitored by
12
13 quadrupole mass spectrometers (QME 220, Pfeiffer Vacuum GmbH; C-100M,
14
15 Leybold-Inficon). The substrate temperature (controlled using a temperature sensor
16
17 PT-100 placed in the sample holder) was systematically varied from -196 °C to room
18
19 temperature during deposition and X-ray diffraction measurement, and the vapour
20
21 pressure of LiCl in a range between 1 and $8 \cdot 10^{-4}$ mbar (calculated from crucible
22
23 temperature). The deposition rates and the deposited layer thicknesses were controlled
24
25 using a quartz crystal monitor (QCM, Inficon). Deposited LiCl was harvested
26
27 quantitatively, and the amount of lithium in the sample was determined by ICP-OES in
28
29 order to calibrate the QCM. Film thicknesses of up to a few hundreds of nanometers
30
31 were achieved. The following materials were used as substrates (all CrysTec GmbH):
32
33 sapphire (0001), ZnO (0001), ZnSe (111), CaF₂ (111), NaCl (111) (all epitaxial
34
35 polished) and cleaved CaF₂ (111). The substrates with the deposited samples were
36
37 transferred from the deposition chamber to an X-ray diffractometer, while maintaining
38
39 vacuum and cooling, by means of a car transfer system.
40
41
42
43
44
45
46
47

48 The powder diffraction patterns were recorded on a θ/θ X-ray powder diffractometer
49
50 (D8-Advance, Bruker AXS) with parallel beam geometry (Goebel mirror, Cu $K\alpha$) in an
51
52 X-ray chamber under ultra high vacuum (ca. $5 \cdot 10^{-8}$ mbar) in reflection mode. The
53
54 chamber is supplied with a slit to absorb scattered radiation which considerably reduces
55
56 the background under vacuum condition from 20° on in 2 θ . Each X-ray pattern was
57
58 monitored at an angle of incidence of 10° using an area sensitive detector (GADDS,
59
60 Bruker AXS). The corresponding pattern was obtained by integration of the two

1
2
3 dimensional diffraction cones. X-ray measurements over the whole sample area
4
5 revealed very low values of local fluctuations. For indexing and structure refinements
6
7 (Rietveld method), the software Topas (Version 3.0, 2006, Bruker AXS) was employed
8
9 [10]. α -LiCl served as an internal standard. Further details on the crystal structure
10
11 investigations can be obtained from the Fachinformationszentrum Karlsruhe, 76344
12
13 Eggenstein-Leopoldshafen, Germany (fax: (+49) 7247-808-666; e-mail: crysdata@fiz-
14
15 karlsruhe.de) on quoting the depository numbers XX.
16
17
18
19
20
21
22
23
24
25
26
27
28
29
30
31
32
33
34
35
36
37
38
39
40
41
42
43
44
45
46
47
48
49
50
51
52
53
54
55
56
57
58
59
60

References

- [1] J. C. Schön, M. Jansen, *Angew. Chem.* **1996**, *108*, 1358; *Angew. Chem. Int. Ed.* **1996**, *35*, 1286.
- [2] M. Jansen, *Angew. Chem.* **2002**, *114*, 3896.
- [3] J. C. Schön, M. Jansen, *Int. J. Mat. Res.* **2009**, *100*, 135.
- [4] D. Fischer, M. Jansen, *Angew. Chem. Int. Ed.* **2002**, *41*, 1755.
- [5] Ž. Čančarević, J. C. Schön, M. Jansen, *Chem. Asian J.* **2008**, *3*, 561.
- [6] D. Fischer, M. Jansen, *J. Am. Chem. Soc.* **2002**, *124*, 3488.
- [7] D. Fischer, A. Müller, M. Jansen, *Z. Anorg. Allg. Chem.* **2004**, *630*, 2697.
- [8] Y. Liebold Ribeiro, D. Fischer, M. Jansen, *Angew. Chem. Int. Ed.* **2008**, *47*, 4428.
- [9] U. Müller, *Anorganische Strukturchemie*, 6. Auflage, Vieweg+Teubner, Wiesbaden 2008, p. 82.
- [10] A. A. Coelho, Topas, General Profile and Structure Analysis Software for Powder Diffraction Data, Version 3.0, Bruker AXS GmbH, Karlsruhe, Germany, 2006.
- [11] W. P. Davey, *Phys. Rev.* **1923**, *21*, 143.
- [12] Determination of the structure candidates by semilocal gradient dependent functional DFT calculation (Becke-PWGGGA), Li and Cl with an all-electron basis set (AEBS).
- [13] G. J. Finch, S. Fordham, *Proc. Phys. Soc.* **1936**, *48*, 85.

Tab.1: Crystallographic data for the Rietveld refinement of LiCl

| | |
|---|--|
| chemical formula | LiCl |
| molar mass [g mol ⁻¹] | 42.4 |
| temperature | -50 °C |
| Cu K _α wavelength, λ [Å] | 1.54059, 1.54449 |
| measured range (2θ) | 11 - 88° |
| R _p [%] ^{a)} | 4.2 |
| R _{wp} [%] ^{a)} | 5.6 |
| <u>β-LiCl</u> | hexagonal |
| space group | <i>P</i> 6 ₃ <i>m</i> c (no. 186) |
| Z | 2 |
| cell parameters [Å] | a = 3.852(1) c = 6.118(1) |
| cell volume [Å ³] | 78.65(4) |
| ρ _{calc} [g cm ⁻³] | 1.8 |
| cry size [nm] | 26.0(2) |
| no. of reflections | 20 |
| Li site | (2b) 1/3, 2/3, 0 |
| Cl site | (2b) 1/3, 2/3, 0.379 ^{b)} |
| preferred orientation | (002): 0.406(2) |
| B _{eq} | 0.2(1) |
| R _{Bragg} [%] ^{a)} | 2.1 |
| <u>α-LiCl</u> | cubic |
| space group | <i>Fm</i> 3̄ <i>m</i> (no. 225) |
| Z | 4 |
| cell parameter [Å] | a = 5.0630(8) |
| cell volume [Å ³] | 129.78(6) |
| ρ _{calc} [g cm ⁻³] | 2.2 |
| cry size [nm] | 24.3(4) |
| no. of reflections | 8 |
| Li site | (4a) 0, 0, 0 |
| Cl site | (4b) 1/2, 1/2, 1/2 |
| preferred orientation | (111): 0.3(1) (022): 0.3(2) |
| B _{eq} | 3.5 |
| R _{Bragg} [%] ^{a)} | 1.9 |

^{a)} R_p, R_{wp}, R_{Bragg} and March-Dollase function for the preferred orientation as defined in

Topas Version 3.0. [10]

^{b)} Unrefined sites, taken from LiBr

1
2
3 **Fig. 1:** E/V curves for selected candidates for low-energy structures discovered by
4 global searches of the LiCl energy landscape, followed by local optimization of each
5 polymorph on the ab initio level ($E_{\text{Min=Wurzite}} = -467.86573$ Hartree) [5, 12]
6
7
8
9

10
11
12 **Fig. 2:** Percentaged crystalline fraction of β -LiCl [wt-%] as determined by Rietveld
13 refinements of the two phase α -/ β -LiCl samples as a function of substrate temperature
14 and vapour pressure of LiCl (calculated from crucible temperature) during deposition
15
16
17

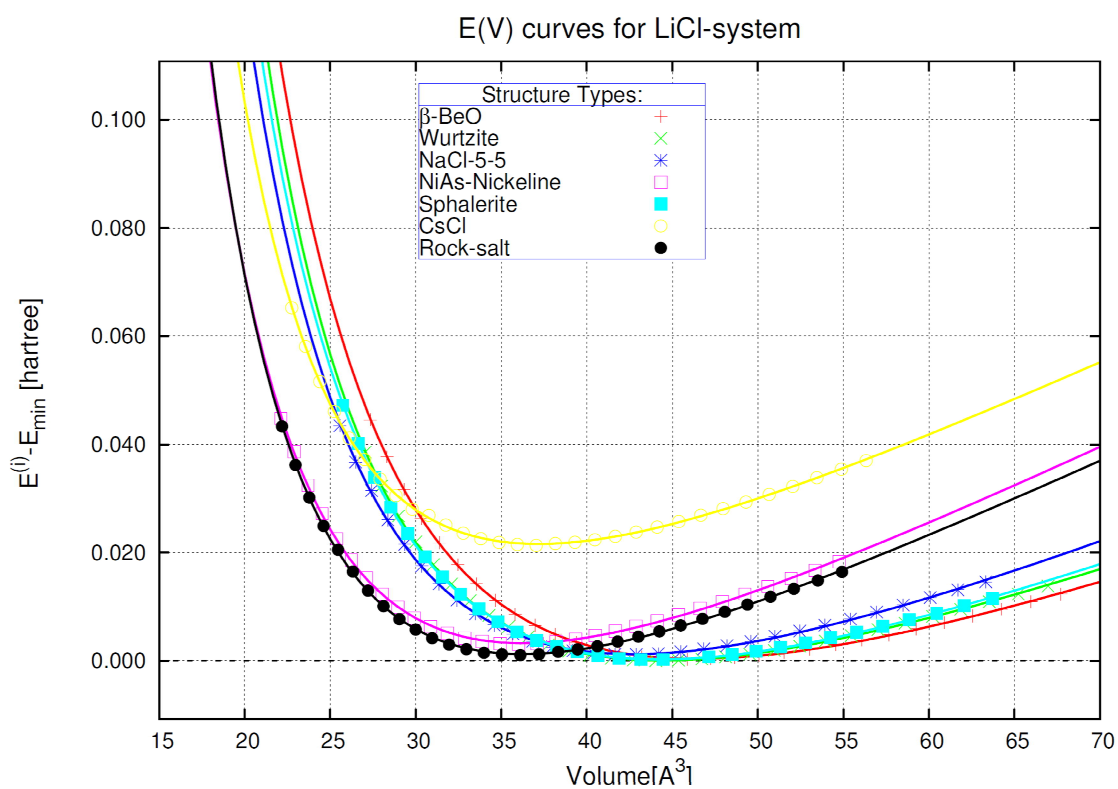
18
19
20
21 **Fig. 3:** X-Ray powder patterns of LiCl (deposited at -50 °C sapphire substrate
22 temperature and $3.7 \cdot 10^{-4}$ mbar LiCl vapour pressure), intensity deviation due to texture,
23 scans from the bottom up: taken at -50 °C (wurtzite and rock salt type), 0 °C (wurtzite
24 and rock salt type) and 25 °C (rock salt type), tick marks: α LiCl
25
26
27
28

29
30
31
32 **Fig. 4:** Rietveld refinement plot of LiCl (deposited at -50 °C sapphire substrate
33 temperature and $3.7 \cdot 10^{-4}$ mbar LiCl vapour pressure), two phase refinement, measured
34 at -50 °C; observed pattern (blue), fitted profile (red), difference profile (grey), tick
35 marks: α -LiCl (black), β -LiCl (green)
36
37
38
39

40
41
42 **Fig. 5:** Cell parameters of wurtzite (left) and rock salt modifications (right) of different
43 lithium halides as determined by Rietveld refinements, LiI (measured at 25 °C) [7],
44 LiBr [8, 13] and LiCl (measured at -50 °C)
45
46
47
48

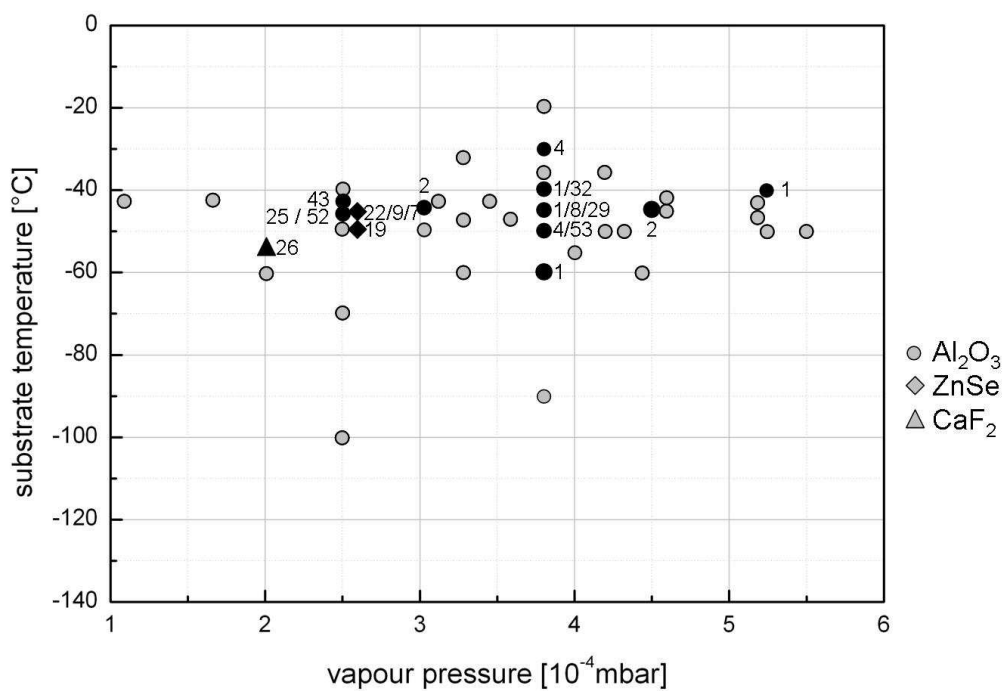
49
50
51 **Fig. 6:** SEM picture showing homogeneity of LiCl surface, 350-fold magnification,
52 deposited at -45 °C sapphire substrate temperature and $3.7 \cdot 10^{-4}$ mbar LiCl vapour
53 pressure, after warming up to 120 °C
54
55
56
57
58
59
60

1
2
3
4
5
6
7
8
9
10
11
12
13
14
15
16
17
18
19
20
21
22
23
24
25
26
27
28
29
30
31
32
33
34
35
36
37
38
39
40
41
42
43
44
45
46
47
48
49
50
51
52
53
54
55
56
57
58
59
60



1
2
3
4
5
6
7
8
9
10
11
12
13
14
15
16
17
18
19
20
21
22
23
24
25
26
27
28
29
30
31
32
33
34
35
36
37
38
39
40
41
42
43
44
45
46
47
48
49
50
51
52
53
54
55
56
57
58
59
60

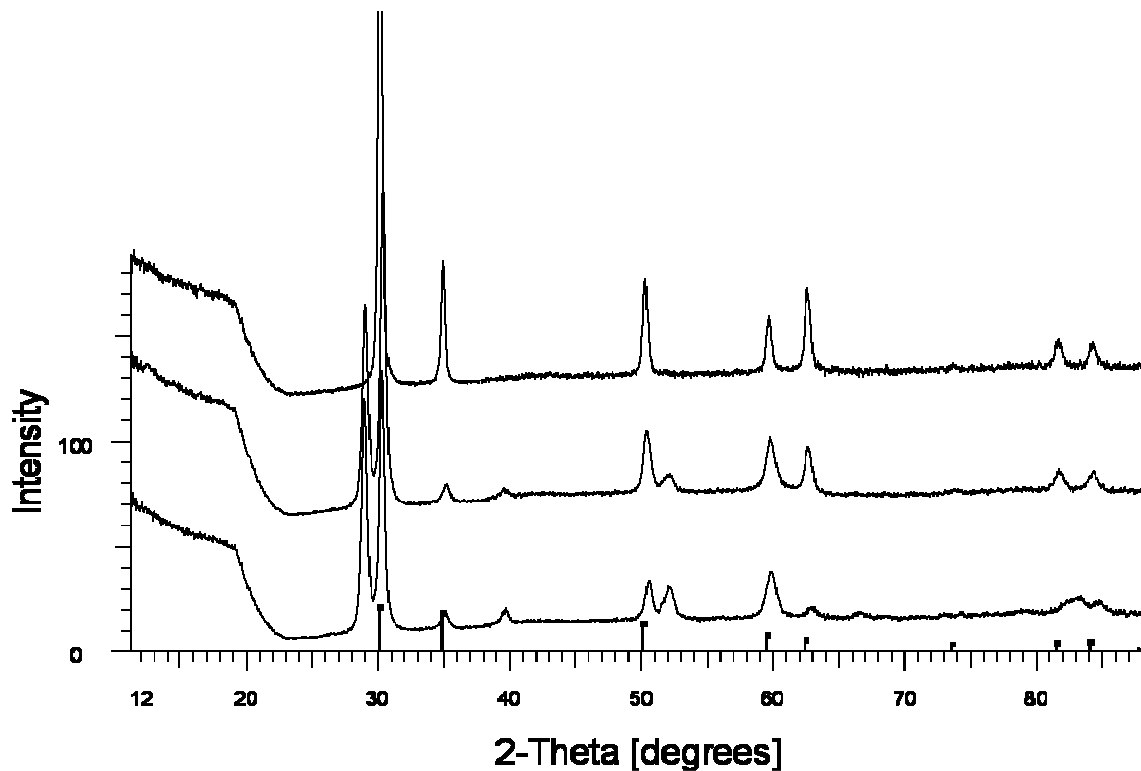
Andreas Bach, Dieter Fischer and Martin Jansen
Fig. 1



1
2
3
4
5
6
7
8
9
10
11
12
13
14
15
16
17
18
19
20
21
22
23
24
25
26
27
28
29
30
31
32
33
34
35
36
37
38
39
40
41
42
43
44
45
46
47
48
49
50
51
52
53
54
55
56
57
58
59
60

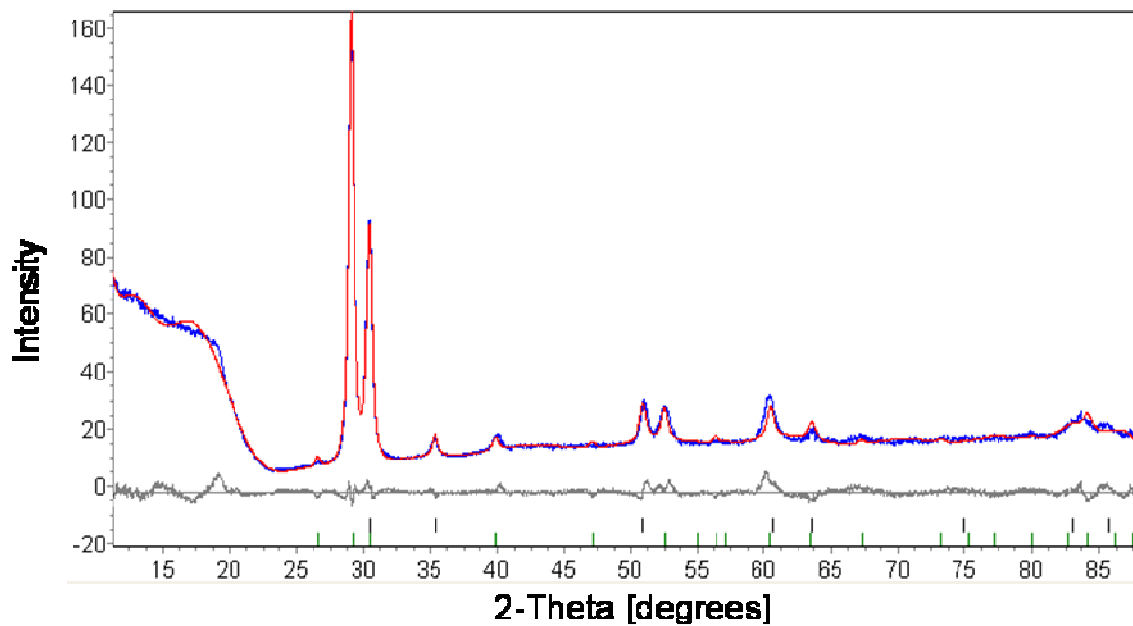
1
2
3
4
5
6
7
8
9
10
11
12
13
14
15
16
17
18
19
20
21
22
23
24
25
26
27
28
29
30
31
32
33
34
35
36
37
38
39
40
41
42
43
44
45
46
47
48
49
50
51
52
53
54
55
56
57
58
59
60

Andreas Bach, Dieter Fischer and Martin Jansen
Fig. 2



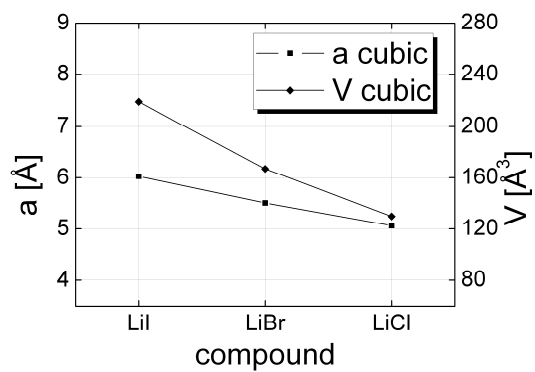
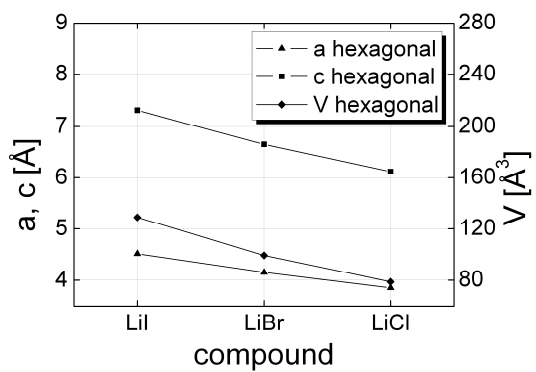
1
2
3
4
5
6
7
8
9
10
11
12
13
14
15
16
17
18
19
20
21
22
23
24
25
26
27
28
29
30
31
32
33
34
35
36
37
38
39
40
41
42
43
44
45
46
47
48
49
50
51
52
53
54
55
56
57
58
59
60

Andreas Bach, Dieter Fischer and Martin Jansen
Fig. 3



1
2
3
4
5
6
7
8
9
10
11
12
13
14
15
16
17
18
19
20
21
22
23
24
25
26
27
28
29
30
31
32
33
34
35
36
37
38
39
40
41
42
43
44
45
46
47
48
49
50
51
52
53
54
55
56
57
58
59
60

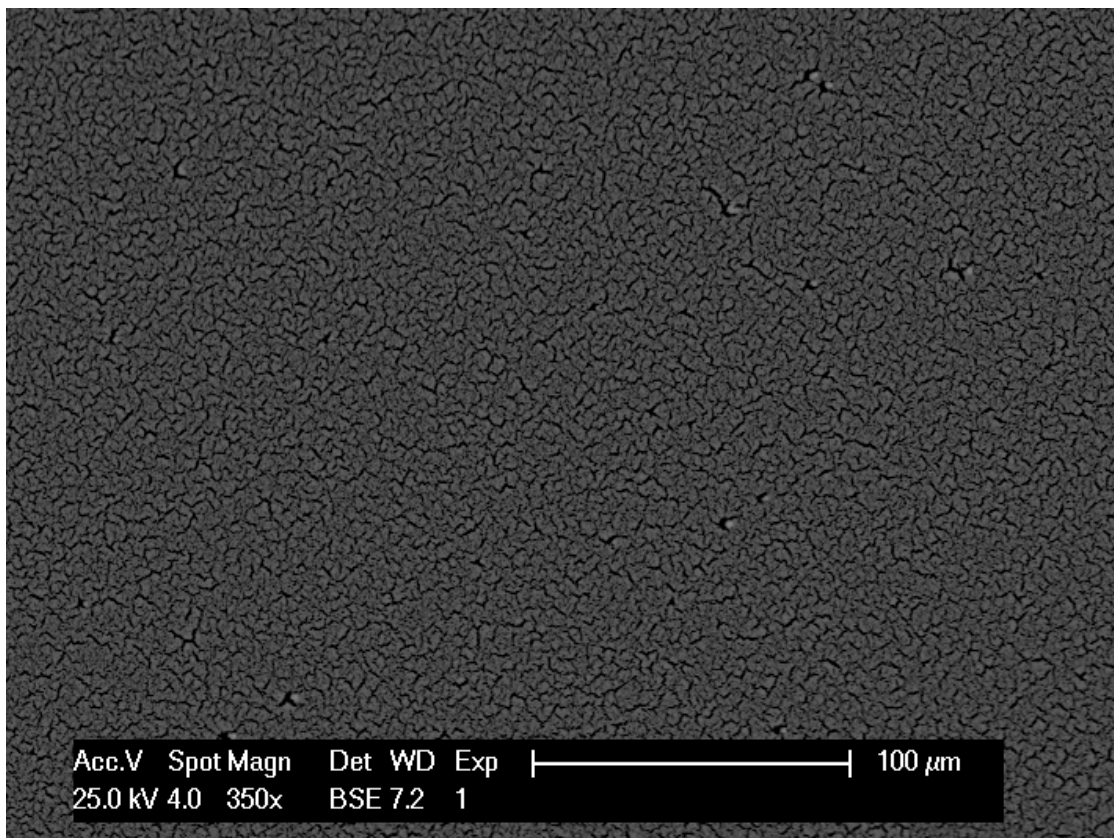
1
2
3 Andreas Bach, Dieter Fischer and Martin Jansen
4 Fig. 4
5
6
7
8
9
10
11
12
13
14
15
16
17
18
19
20
21
22
23
24
25
26
27
28
29
30
31
32
33
34
35
36
37
38
39
40
41
42
43
44
45
46
47
48
49
50
51
52
53
54
55
56
57
58
59
60



1
2
3
4
5
6
7
8
9
10
11
12
13
14
15
16
17
18
19
20
21
22
23
24
25
26
27
28
29
30
31
32
33
34
35
36
37
38
39
40
41
42
43
44
45
46
47
48
49
50
51
52
53
54
55
56
57
58
59
60

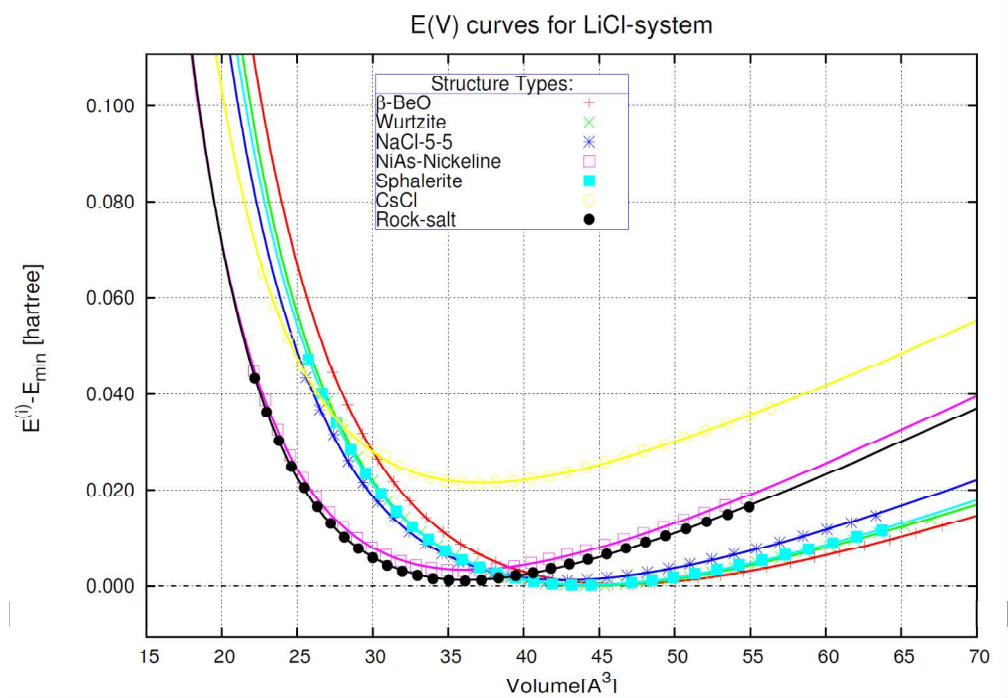
Andreas Bach, Dieter Fischer and Martin Jansen
Fig. 5

1
2
3
4
5
6
7
8
9
10
11
12
13
14
15
16
17
18
19
20
21
22
23
24
25
26
27
28
29
30
31
32
33
34
35
36
37
38
39
40
41
42
43
44
45
46
47
48
49
50
51
52
53
54
55
56
57
58
59
60

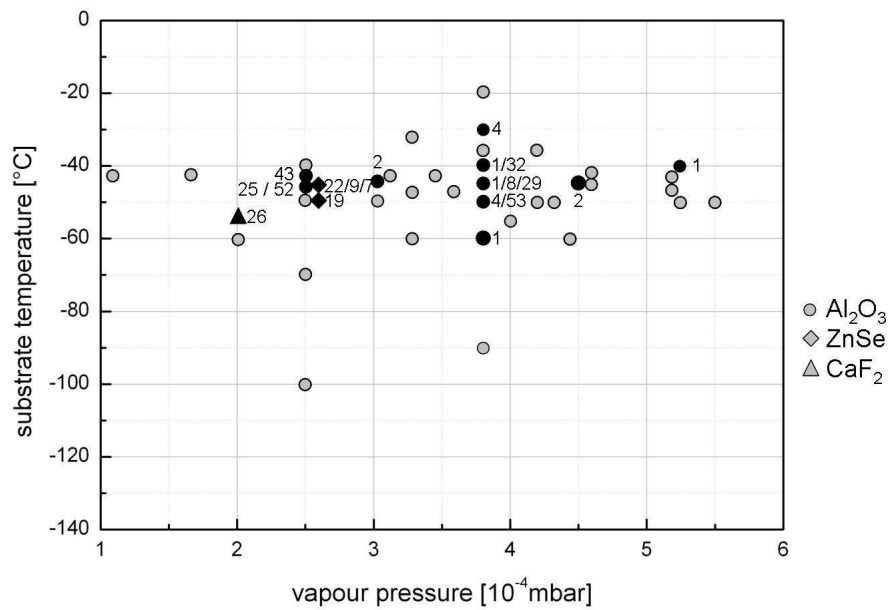


1
2
3 Andreas Bach, Dieter Fischer and Martin Jansen
4 Fig. 6
5
6
7
8
9
10
11
12
13
14
15
16
17
18
19
20
21
22
23
24
25
26
27
28
29
30
31
32
33
34
35
36
37
38
39
40
41
42
43
44
45
46
47
48
49
50
51
52
53
54
55
56
57
58
59
60

1
2
3
4
5
6
7
8
9
10
11
12
13
14
15
16
17
18
19
20
21
22
23
24
25
26
27
28
29
30
31
32
33
34
35
36
37
38
39
40
41
42
43
44
45
46
47
48
49
50
51
52
53
54
55
56
57
58
59
60



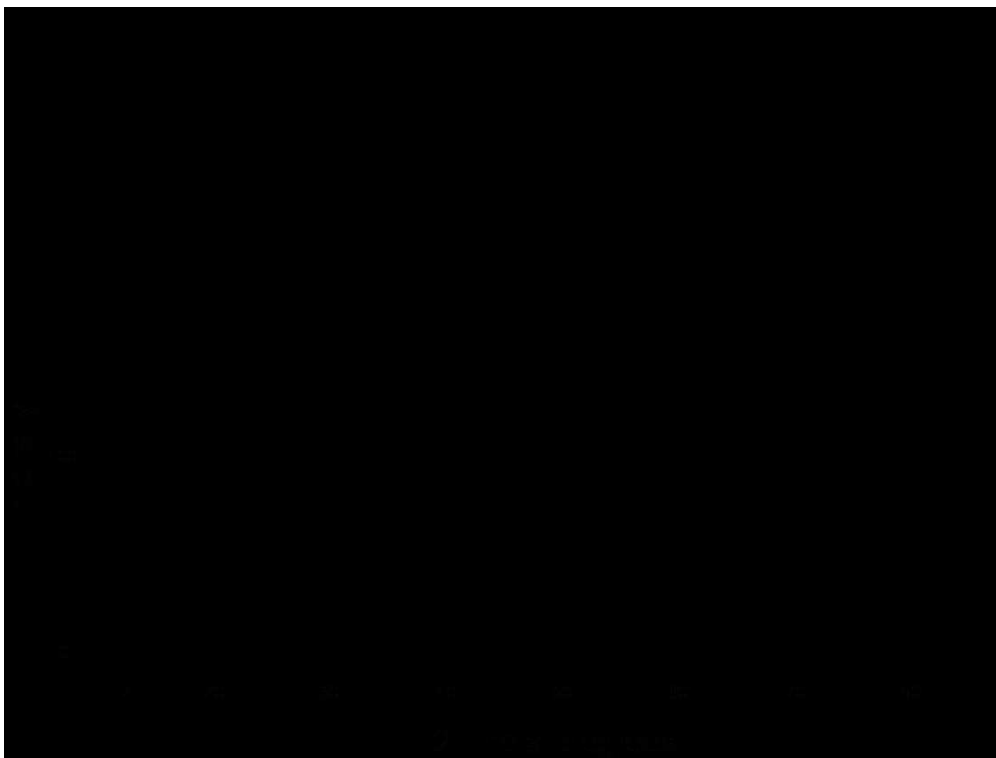
1880x1321mm (96 x 96 DPI)



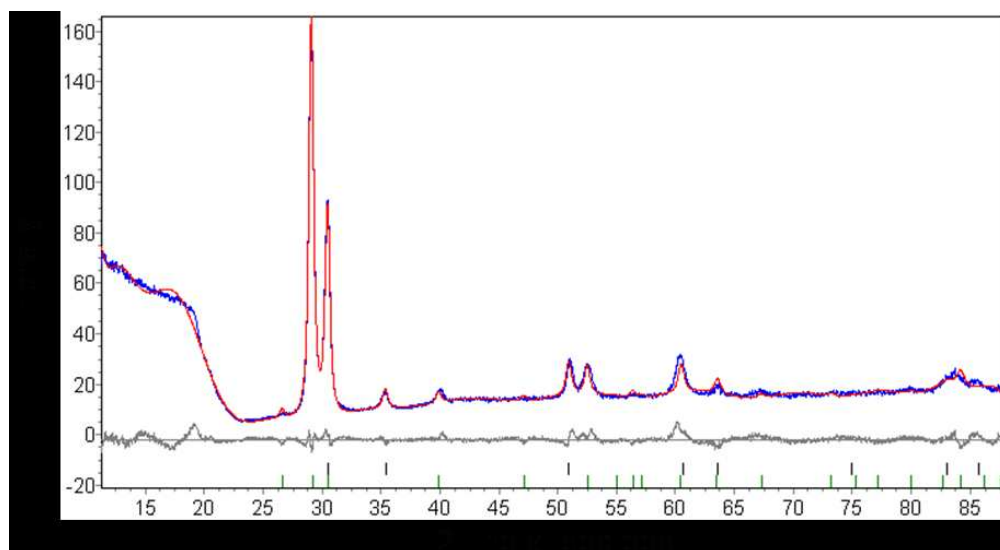
254x179mm (150 x 150 DPI)

1
2
3
4
5
6
7
8
9
10
11
12
13
14
15
16
17
18
19
20
21
22
23
24
25
26
27
28
29
30
31
32
33
34
35
36
37
38
39
40
41
42
43
44
45
46
47
48
49
50
51
52
53
54
55
56
57
58
59
60

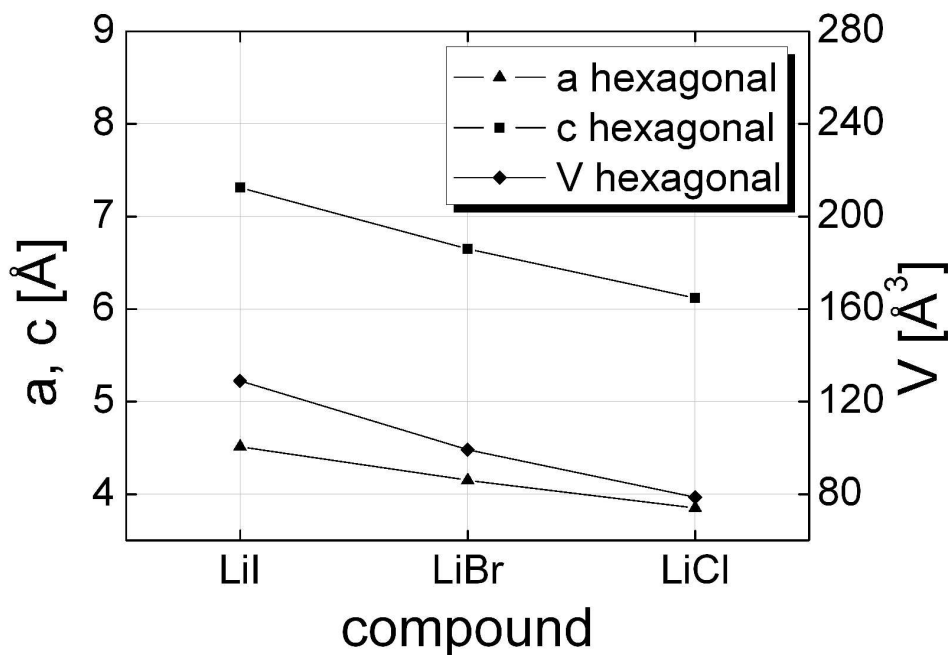
1
2
3
4
5
6
7
8
9
10
11
12
13
14
15
16
17
18
19
20
21
22
23
24
25
26
27
28
29
30
31
32
33
34
35
36
37
38
39
40
41
42
43
44
45
46
47
48
49
50
51
52
53
54
55
56
57
58
59
60



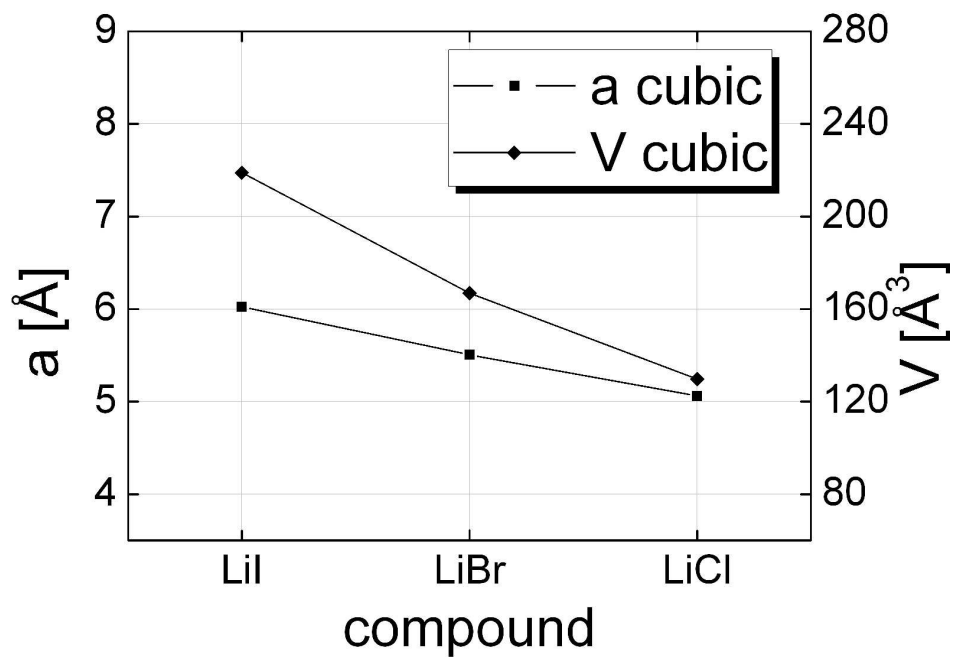
278x198mm (102 x 108 DPI)



154x84mm (150 x 150 DPI)



287x203mm (300 x 300 DPI)



287x203mm (300 x 300 DPI)

1
2
3
4
5
6
7
8
9
10
11
12
13
14
15
16
17
18
19
20
21
22
23
24
25
26
27
28
29
30
31
32
33
34
35
36
37
38
39
40
41
42
43
44
45
46
47
48
49
50
51
52
53
54
55
56
57
58
59
60

